

# What criticality in cellular automata models of earthquakes?

Silvia Castellaro and Francesco Mulargia

Settore di Geofisica, Dipartimento di Fisica, viale Bertoni Pichat 8, 40127 Bologna, Italy.  
E-mails: [silvia@ibogeo.df.unibo.it](mailto:silvia@ibogeo.df.unibo.it); [mulargia@ibogfs.df.unibo.it](mailto:mulargia@ibogfs.df.unibo.it)

Accepted 2002 February 19. Received 2001 June 22; in original form 2002 February 11

## SUMMARY

Six different 2-D prototype cellular automata models are developed to analyse the main variants of the massless automata proposed so far to reproduce earthquake physics. The analysis aims at identifying the existence of features common to these models, if any. The different model variants were studied with regard to: (1) initial grid configuration, homogeneous or random heterogeneous; (2) loading function, random or uniform; (3) local dissipation; (4) local redistribution. As a first general result, it is found that the models exhibit criticality over a very restricted range of spatial scales, much smaller than that imposed by the geometrical dimensions of the grid alone. The latter, in contrast, governs the initial transient dynamics, which exhibits much larger events. As a second general result, the foreshocks are found to increase systematically in both rate of occurrence and size prior to main shocks, with a simultaneous progressive deficit of small events. This, in turn, implies an increase in correlation length and a ‘precursor’ decrease in the  $b$ -value. As a third general result, the presence of foreshocks in cellular automata and the difficulties in detecting them in real earthquakes still only give a limited applicability of the present cellular automata models to the real world. As a final general result, periodic recurrence of main shocks is found only for locally dissipative models.

**Key words:** cellular automata, criticality, earthquakes.

## 1 INTRODUCTION

In physics, a critical point is defined as a point at which a system radically changes its behaviour or structure at all scales. This shows up as a power-law distribution of the fundamental observables. In general, some parameters of the system must be tuned to achieve critical behaviour. A particular case is that of self-organized critical systems (Bak & Tang 1989), which reach their critical state by self-tuning their intrinsic dynamics.

The Gutenberg–Richter law (Gutenberg & Richter 1954) for earthquakes, spanning over at least five decades, is one of the best examples of power-law behaviour in natural phenomena and it has often been interpreted as proof of the fact that the Earth’s lithosphere is a critical, possibly self-organized, system. This issue has been corroborated by the findings of the many cellular automata models that have been developed. However, most of these models have common features and it is not known to what extent this coincidence of the results is a result of common premises. Lomnitz-Adler (1993) examined 40 variants of cellular automata focusing on their capability to reproduce a Gutenberg–Richter-type power-law distribution. His study was performed on automata of small dimensions, generally  $24^2$ ,  $32^2$ ,  $48^2$  and only occasionally  $64^2$  elements. In our previous work (Castellaro & Mulargia 2001) we noted how such small sizes (particularly grids up to  $40 \times 40$  cells) can substantially affect the observed properties.

In this paper, we focus our attention on the effect of the common premises adopted by the principal automata that have been

proposed by using grids large enough to avoid the most obvious size effects. To start with, all models appear to be based on more or less homogeneous grids of elements for which a threshold level for cell failure can be reached by ‘loading’ the sample. When a failure event occurs at a cell, the load is redistributed to its neighbours. The rules governing such transitions can be defined *a priori* or derived from constitutive equations. The latter is the case when the cells are defined as harmonic oscillators with masses connected by elastic springs. In the present work we will only consider massless cellular automata, since they are more flexible in representing intrinsic nonlinearities. As regards the premises of massless cellular automata, we will investigate the consequences of:

- (1) the starting configuration, namely the initial state of the grid elements, which can be *homogeneous* or *heterogeneous*;
- (2) the loading function, that is the rules according to which the grid is loaded – we will discuss *random* and *uniform* loading;
- (3) the *local energy dissipation*, which mimics the effect of frictional heat loss on real faults;
- (4) the *local redistribution* accompanying cell failure.

In our analysis we use square grids of fixed dimension, of  $10^4$  cells. This is a size easily manageable by normal computers and large enough to avoid all the obvious instabilities of some parameters, such as the average dimension of the main shocks and the number of foreshocks and aftershocks with respect to the main shock, which are most sensitive to small grid sizes. Note how this does not dissipate all doubts concerning the grid size dependence. However, studying

this problem *ab initio* has so far proven to be prohibitive even for the most powerful parallel machines (Kinouchi & Prado 1999).

The models we analyse do not exhaust the range of cellular automata presented in the literature (see e.g. Steacy & McCloskey 1998).

## 2 THE MODELS

We perform our analysis by means of six different prototype cellular automata models, which are designed to incorporate the basic features of the massless cellular automata presented so far. As anticipated, ‘massy’ cellular automata are not discussed in this paper because of their inferior flexibility as well as to avoid all complications introduced by the numerical treatment they require, which may confound the basic physical issues. The basis for cellular automata models, which are all related to the original (Bak & Tang 1989) paradigm, is a 2-D square grid of cells, which can be thought of representing both a fault surface and the projection of a hypothetical set of faults on the Earth’s surface. ‘Particles’ representing energy, stress or strain or, more generally, *ruptini* (unit of increase in the ‘strain’ level of a cell or unit of decrease in the threshold value for its failure, cf. Castellaro & Mulargia 2001) are added to the grids according to some prescribed rules until the failure value is reached at some cell. This event is taken as a rupture and starts the redistribution of the ruptini lost from the ‘broken’ element to its neighbours, according to other prescribed rules. This redistribution can lead other cells to instability and continues in a cascade until the whole grid is stable again. The number of cells that fail constitutes the event size.

Our aim is to investigate the extent to which the different constitutive rules of the principal cellular automata presented in the literature lead to common properties, especially those related to self-organization. We have therefore built six different prototype models that differ in the initial state of the cells, in the method and amount of loading, in the redistribution rules and in the energy lost by each failing cell.

The first model is a basic automaton of Bak–Tang type, involving just the nearest neighbours in the redistribution of ruptini after cell failure. The second one shows larger interactions: after the rupture of a cell, the energy redistribution around it involves a larger neighbourhood and the system is conservative. The third model considers long-range interactions as the second one but it is non-conservative, with a small amount of energy lost locally from the grid at each redistribution. The fourth model mimics the third one for the long-range interactions and the local dissipation but energy redistribution is ‘smoother’. The fifth model is again non-conservative and with long-distance interactions but the amount of dissipation is about eight times larger than in the third model. The last model is also non-conservative and with long-range interactions but it is built on a heterogeneous grid.

Let us now describe these variants in detail.

(1) Small-neighbourhood (SN) model. This model mimics the Bak & Tang redistribution and loading (Bak & Tang 1989).

*Neighbourhood*: only the four nearest neighbours to the unstable cell are involved in the redistribution, that is

$$\begin{aligned} \text{if } N(i, j) \geq \tau \text{ then} \\ N(i, j) &= N(i, j) - \tau \\ N(i \pm 1, j) &= N(i \pm 1, j) + \tau/4 \\ N(i, j \pm 1) &= N(i, j \pm 1) + \tau/4, \end{aligned} \quad (1)$$

where  $N(i, j)$  is the state of the  $(i, j)$  element of the system and  $\tau$  is the threshold level for rupture.

*Initial grid condition*: the grid is initially empty.

*Loading function*: a ruptino is randomly added to the grid at each time step.

*Dissipation*: no energy is dissipated from the unstable elements, apart from the grid borders.

(2) Large-neighbourhood (LN) model. In this model, energy redistributions from each unstable element involves a number of neighbours larger than the SN model and in a time-dependent way.

*Neighbourhood*: at  $t = 0$  such as in eq. (1) and at the successive time steps (namely at the successive iterations),

$$\begin{aligned} t = 1, \quad N(i, j) &= N(i, j) - \frac{2}{3}\tau \\ N(i \pm 1, j \pm 1) &= N(i \pm 1, j \pm 1) + \tau/6 \end{aligned} \quad (2)$$

$$\begin{aligned} t = 2, \quad N(i, j) &= N(i, j) - \tau/3 \\ N(i \pm 2, j) &= N(i \pm 2, j) + \tau/12 \\ N(i, j \pm 2) &= N(i, j \pm 2) + \tau/12 \end{aligned} \quad (3)$$

$$\begin{aligned} t = 3, \quad N(i, j) &= N(i, j) - \tau/3 \\ N(i \pm 1, j \pm 2) &= N(i \pm 1, j \pm 2) + \tau/12 \\ N(i \pm 2, j \pm 1) &= N(i \pm 2, j \pm 1) + \tau/12. \end{aligned} \quad (4)$$

The rationale for this model and its details are described in Castellaro & Mulargia (2001).

*Initial grid condition*: the grid is initially empty, i.e. all cells are set at a zero level.

*Loading function*: a ruptino is injected at a uniformly random position of the grid at each time step.

*Dissipation*: no energy is locally dissipated from unstable cells. Dissipation only occurs at the grid borders that are totally lossy, in the sense that all ruptini redistributed at borders are lost.

(3) Small-dissipation, large-neighbourhood (SDLN) method.

*Neighbourhood*: it involves all four successive sets of nearest neighbours as described in the LN model above.

*Initial grid condition*: the grid is initially empty.

*Loading function*: a ruptino is injected at a random position at each time step.

*Dissipation* one ruptino is locally dissipated from each unstable cell.

(4) redSDLN. Identical to SDLN but with different redistribution rules for the unstable elements. The differences in the level between the broken and the surrounding elements are smaller.

*Neighbourhood*: it involves all four successive sets of neighbours as described in the LN model above but with a reduced ‘strain’ difference between the ruptured element and its nearest neighbours. The transition rule at the first stage after rupture ( $t = 0$ , eq. 1), becomes:

$$\begin{aligned} \text{if } N(i, j) \geq \tau \text{ then} \\ N(i, j) &= N(i, j) - \tau \\ N(i \pm 1, j) &= N(i \pm 1, j) + \tau/6 \\ N(i, j \pm 1) &= N(i, j \pm 1) + \tau/6. \end{aligned} \quad (5)$$

*Initial grid condition*: the grid is initially empty.

*Loading function*: a ruptino is injected at a random position at each time step.

*Dissipation*: it follows from the transition rules governing the first time step, that four ruptini are locally dissipated at each unstable cell.

**Table 1.** Summary of the properties of the models studied.

Model	Neighbours	Starting grid	Loading function	Dissipation
SN	Four nearest neighbours	Empty	Random	None
LN	21 nearest neighbours	Empty	Random	None
SDLN	21 nearest neighbours	Empty	Random	One ruptino (10 per cent energy)
redSDLN	21 nearest neighbours	Empty	Random	One ruptino but smoothed laws
LDLN	21 nearest neighbours	Empty	Random	66 per cent energy
LDLNEt	21 nearest neighbours	Heterogeneous	Uniform	66 per cent energy

(5) Large-dissipation, large-neighbourhood (LDLN) model. In this model all four successive rims of neighbours are involved in the redistribution of energy from the unstable cells and the amount of dissipation is high. The transition rules are those explained in the LN model.

*Neighbourhood:* as in the LN model.

*Initial grid condition:* the grid is initially empty.

*Loading function:* a ruptino is injected at a random position at each time step.

*Dissipation:* eight ruptini are locally dissipated at the originally unstable cell.

(6) LDLNEt. Follows the redistribution rules given for the LN model but with different initial grid conditions and a large dissipation level.

*Neighbourhood:* as in the LN model.

*Initial grid condition:* each cell of the grid is initially randomly loaded with a number of ruptini ranging from 0 to the threshold level for rupture  $\tau$ .

*Loading function:* a ruptino is added to each cell at each time step.

*Dissipation:* eight ruptini are lost from the originally unstable cell.

A summary of the parameters associated with the different models is reported in Table 1.

### 3 THE MEAN ENERGY

The mean energy of a system is a variable that efficiently illustrates, when it exists, the procedure of self-organization (Rundle *et al.* 1999). In all the cases we analysed, the mean energy, defined as being proportional to the square of the cell level averaged over the whole grid, shows a first transient during which the system is not under stationary conditions, and then tends towards an equilibrium value. For all the non-dissipative automata, we find that this value is constant while in the locally dissipative ones oscillations are present that are proportional to the degree of local dissipation. For highly dissipative systems the evolution is very slow and even after  $40 \times 10^6$  iterations the system does not reach a stationary dynamics.

As we can see from Fig. 1, after the initial linear increase in the mean energy (which is proportional to the strain squared) owing to the loading rules that prescribe that the system should start from an empty grid, the systems SN and LN do not show any oscillation in the mean energy. As expected from the time-domain series, the energy power spectra do not exhibit significant peaks for any of the locally non-dissipative systems. Spectral analysis has been performed via

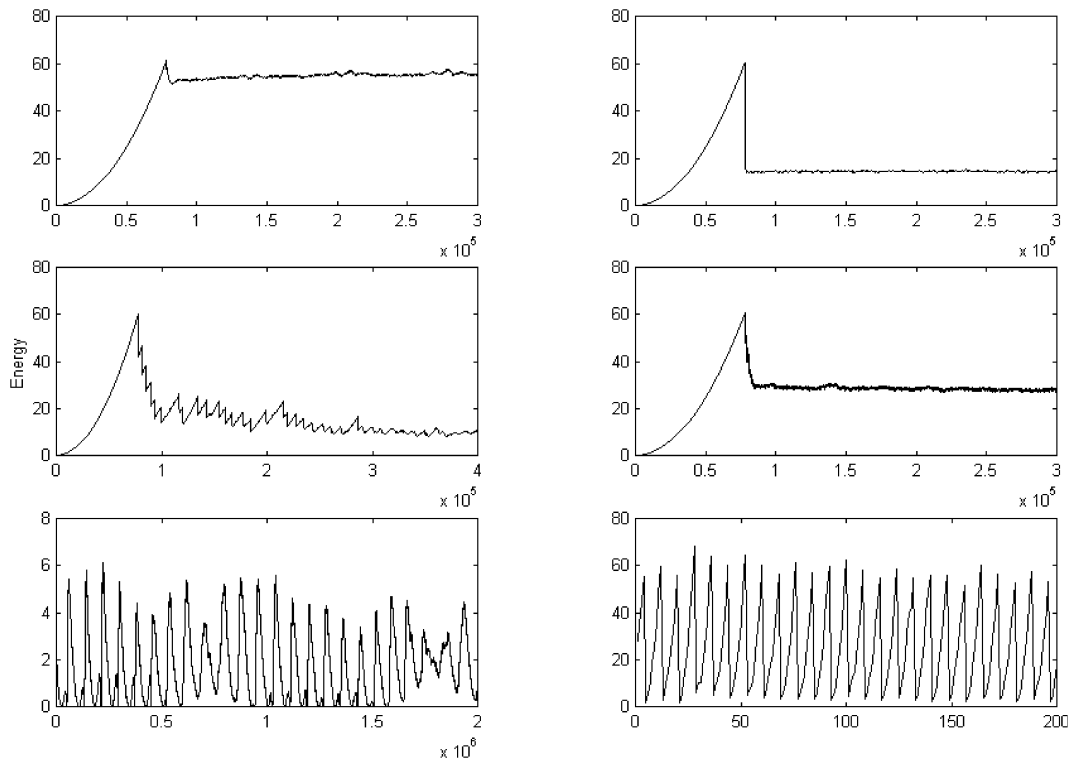


**Figure 1.** Cell averaged energy in the prototype models during their evolution. Energy ( $y$ -axis) is expressed in ruptino<sup>2</sup> units (see text). Time ( $x$ -axis) is expressed in number of iterations. From the top left to the bottom right, the plots show, in order, the SN, LN, SDLN, redSDLN, LDLN and LDLNEt models (see text).

**Table 2.** The most significant peaks in the power spectra for the average energy of the different models. The period is given in number of iterations. The significance for each peak is evaluated in terms of the ratio  $\bar{g}/g$ , which increases with the peak significance.  $g = 1 - e^{(\log p - \log m)/m}$ , where  $m$  is the number of data divided by 2 and  $p$  is the threshold level for significance taken at 1 per cent.  $\bar{g} = V^2/2s^2$  in which  $V$  is the amplitude of the peak and  $s$  is the sum of the powers at each frequency.

Model	Period	Peak significance ratio related to the 1 per cent critical value
SN	None	—
LN	None	—
SDLN	$T_1 = 74\,898$	$\bar{g}/g_{0.01} = 540$
redSDLN	$T_1 = 262\,144$	$\bar{g}/g_{0.01} = 526$
	$T_2 = 87\,381$	$\bar{g}/g_{0.01} = 302$
LDLN	$T_1 = 209\,715$	$\bar{g}/g_{0.01} = 75$
	$T_2 = 131\,072$	$\bar{g}/g_{0.01} = 37$
	$T_3 = 104\,858$	$\bar{g}/g_{0.01} = 29$
LDLNet	$T_1 = 8$	

fast Fourier transform using a Welch window after detrending the data, which had been previously piecewise linearly interpolated.

As pointed out by Sammis & Smith (1999), Main *et al.* (2000) and Castellaro & Mulargia (2001), the picture for the dissipative systems is different. In this case, the mean energy has an apparent oscillation in time, which is a result of a sort of shadow left behind by large events. Calling  $f$  the fraction of energy lost, that is  $1/r$ , where  $r$  is the number of ruptures lost by local dissipation, the period  $T$  of the oscillation increases with decreasing  $f$  as  $T \propto f^{-1}$ .

The spectral analysis performed on the energy time-series clearly shows some significant peaks, which are summarized in Table 2

and shown in Fig. 2. As we can see from the table, the higher the local dissipation, the longer the period of oscillation shown by the automata. It also emerges that the most complex behaviour, namely that with many frequency peaks, occurs for models in which a large neighbourhood is involved in the redistribution following the failure of a cell. Since in the real Earth the region affected by an earthquake in terms of strain redistribution is likely to have a complex geometry, this could be taken as a possible explanation for the fact that no periodicity is observed in earthquake sequences. The sharp periodicity displayed by the LDLNet model was expected since this model is based on a homogeneous loading of a random heterogeneous basis.

In our exploration of the dependence of the results on parameter tuning, we have first of all to face the problem of the definition of criticality. The correlation length, which is the ‘size’ of the maximum cluster in a given system, is by definition infinite at the critical point, where clusters of all dimensions occur. The correlation length is linked to the maximum size of rupture events, and therefore the latter provides a direct measure of criticality. The mean energy is expected to increase with correlation length, although the former can also increase owing to many smaller and uncorrelated ruptures. Provided that the first hypothesis is correct, one may expect that, if the energy is constant, the correlation length also remains constant and if its maximum value coincides with the maximum possible for the system, a critical state has been reached. Note also how, in this case, since there is no external parameter tuning, this should be interpreted as self-organized criticality.

This issue has to face some practical difficulties since, owing to present limitations in computing power, scale-invariant behaviour in cellular automata models can only be verified over two orders of magnitude at most. Therefore, any issue of criticality must rely

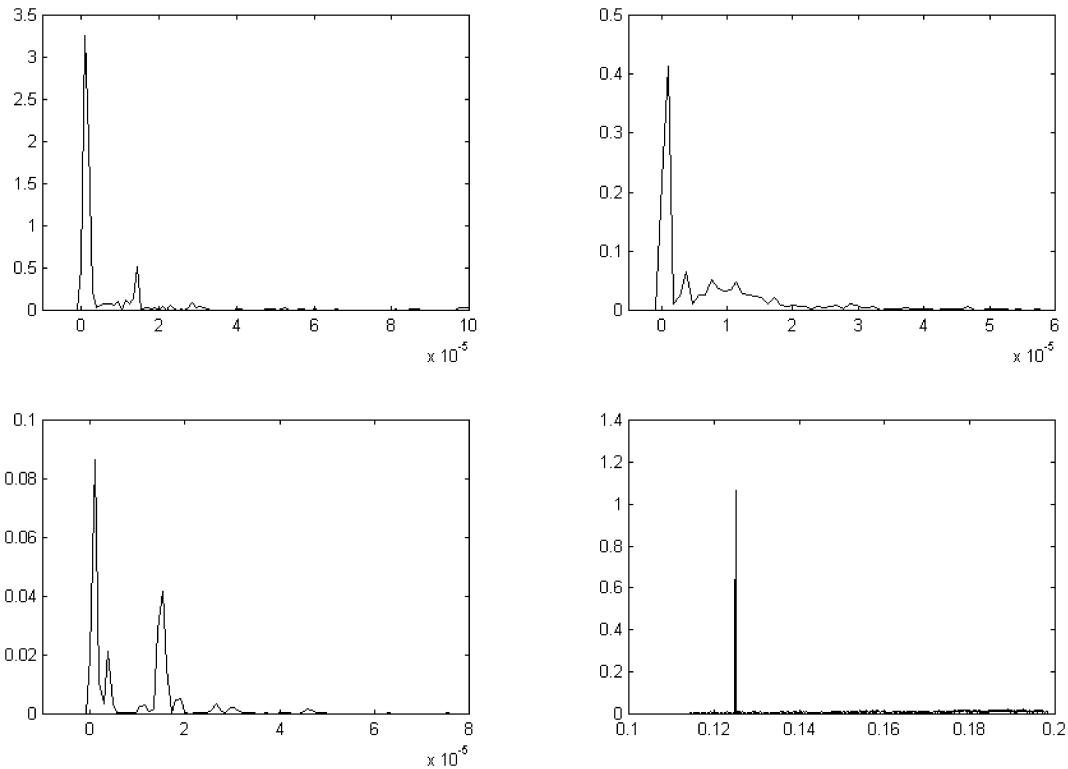


**Figure 2.** Power spectra of the average energy in the non-conservative prototype models. The frequencies ( $x$ -axis) are expressed in iteration $^{-1}$  units, while the peak amplitude ( $y$ -axis) is in arbitrary units. From the top left to the bottom right, the spectra show, in order, the SDLN, redSDLN, LDLN and LDLNet models. The conservative models do not show any significant peak and their spectra are not represented here.

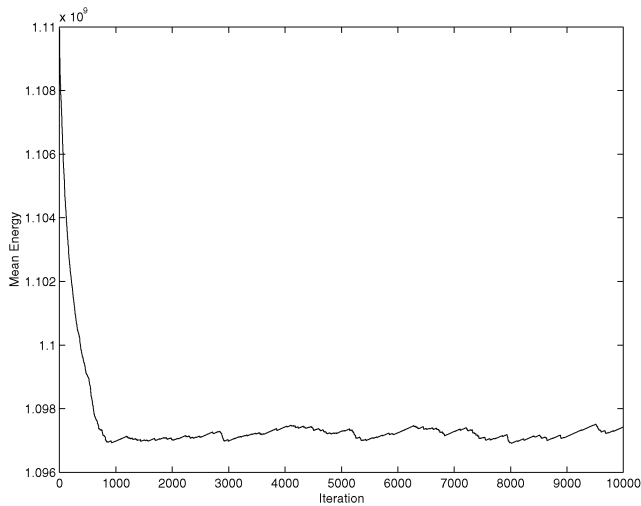


**Figure 3.** In an initially randomly heterogeneous LN system, the energy level decreases a little with the evolution of the system according to the established rules. This implies that some order does emerge.

on large extrapolations of what can be seen on such a restricted range.

In practice, what we generally observe is that the mean value around which the systems stabilize is not the maximum geometrically possible for that grid. During the initial transient stage of the automata dynamics, as apparent from Fig. 1, the average energy is much higher than in the following, and the same is true for the event sizes. Barring the SN model, which has a simple redistribution rule and no local dissipation and which shows a modest average grid energy decrease with respect to the initial transient value (Fig. 1), all other models show a mean energy after the initial transient, which is only about 50 per cent of that attained during the first initial transient.

A similar behaviour is apparent, irrespective of local dissipation, if the grid starts from a random heterogeneous state (Fig. 3). This is remarkable since it indicates that the system stabilizes in a state, which is far from being both homogeneous and random heterogeneous.

A basic question is in order here: is it more appropriate to represent the fault, or a portion of lithosphere, with the transient or the subsequent ‘stationary’ dynamics? The answer is not obvious, since stationary dynamics is favoured by the trivial tectonic arguments of long evolutionary timescales, while transient dynamics is favoured by the fact that the transient interval lasts for a very large number, typically  $10^5$ , of system-size events.

Under the hypothesis of accepting both the stationary hypothesis as well as that of ‘criticality’, if the Earth’s crust were really in a state similar to that described by the dissipative automata, then it would not be in a state of continuous self-organized criticality. This issue of approach and retreat from a critical dynamics has been somehow suggested to coincide with a feature of real earthquakes. Jaumé & Sykes (1999) and Jaumé (2000), studying the last large North American earthquakes, apparently recognized an increase in the rate of energy release prior to the main events. This would imply that the lithosphere is not always ready to break with the maximum possible events but that the strain-energy level needs to increase, incrementing the correlation length, up to a critical point, which therefore would be, in principle, predictable.

We recall here that both organized criticality and self-organized criticality must be referred to sufficiently long periods of time in

which a system can show a ‘stable’ metastability, and therefore this issue is tied to the observation time with respect to the timescale of the process. Also in this case, as in that of transient/stationary dynamics, there seems to be no obvious answer. The reason lies in the fact that cellular automata models have an evolution time, which cannot be directly tied to that of real phenomena. This means that an iteration cycle may correspond to seconds, days or months at various points of the simulation. In any case, some insight concerning the features of a possible intermittent criticality can be gathered by the following arguments.

#### 4 THE MAINSHOCKS

The constancy of the mean grid energy and the constancy of the mainshock size would suggest that the system has reached a ‘critical’ condition, even if the values attained are much lower than those corresponding to the maximum geometrically possible in the system. Further insight on this point can be gathered from the time-series of the mainshocks and of the foreshocks. In Figs 4 and 5 we report the picture of all the event (fore-, main- and aftershocks) time-series and that of the mainshocks alone for non-dissipative and dissipative cases. The initial non-stationarity owing to the loading function and to the initially homogeneous empty grid has been removed in the former case. Note that, in the non-dissipative models, the maximum mainshock size is approximately constant.

In order to check whether an intermittent criticality (periodic or not) exists in these systems, we have studied the interevent times between mainshocks. The distribution of these time intervals is also found to be power law (Fig. 6). Its spectral analysis (Fig. 7) shows no significant peak for any of the models analysed except for LDLNet. We considered only the sequences of the largest 20 per cent of mainshocks because we aimed to mimick the generalized interest in the largest earthquakes. However, no substantial difference was found by lowering the threshold values. The reason for the ‘anomalous’ behaviour of the LDLNet model appears again owing to the uniform load and the consequent cyclical rupturing.

The latter results are in partial agreement with those of Sammis & Smith (1999), who found a perfectly regular periodicity in their interevent times of a uniform homogeneous automaton with local dissipation. Our LDLNet model, which is very similar to the model used by these authors except for the extended local redistribution, presents a similar regularity, albeit less evident. The perfect regularity found by Sammis & Smith (1999), should then be traced to their very simple redistribution scheme, which is limited to the nearest neighbours alone.

#### 5 FORESHOCK PROPERTIES

According to the definition we gave in our previous work (Castellaro & Mulargia 2001) we define a cluster as an uninterrupted series of ruptures within which the mainshock is the largest event. The rupture events preceding it in the same cluster are its foreshocks and those following it are its aftershocks. Note how this definition does not totally match the seismological definition of foreshocks, which means events correlated in time and hypocentre to the mainshock. Our definition is dictated by the lack of an absolute timescale in the cellular automata (*cf.* above), where time is only represented by an iteration number and where the small grid size implies that all the events on the grid are correlated.

It has been proposed by several authors that earthquakes do not occur completely at random but rather follow some specific patterns. Changes in the rate of seismic moment or energy release before a

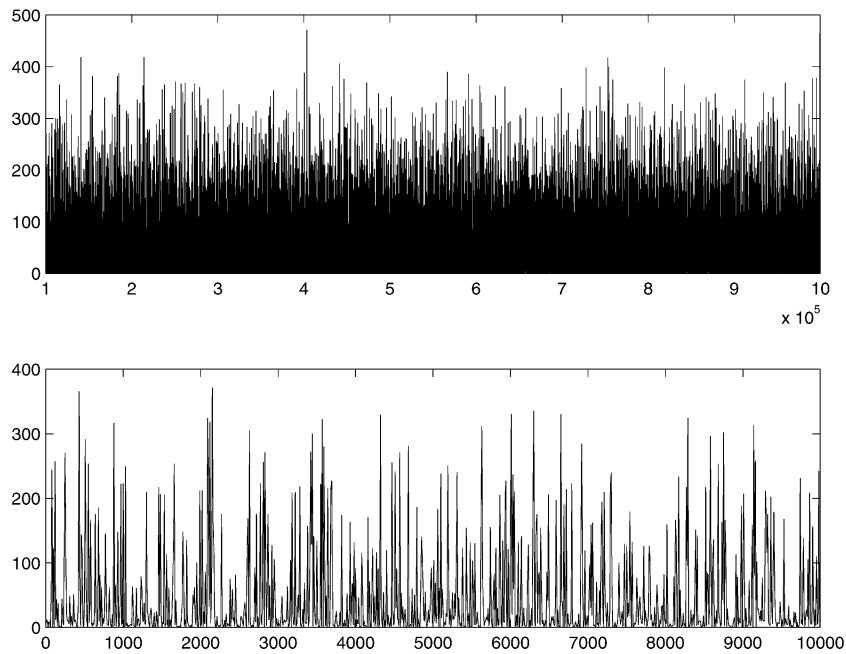


**Figure 4.** Time-series of all the events (top) and of the mainshocks sampled each 10 events (bottom) in  $10^6$  iterations of a LDLN model under stationary conditions (see text). Note that mainshock size is stationary.

big earthquake have often been suggested. Bufe & Varnes (1993), Jaumé & Sykes (1999) and Jaumé (2000) claim that, at least for the (mostly North American) earthquakes they have studied, the cumulated magnitude–frequency distributions for the largest events show a change in slope. In particular, the slope decreases, indicating an increasing number of large events while approaching the mainshock. This is consistent with the critical point hypothesis of a correlation-length increase (Rundle *et al.* 1999). It should be noted that similar, although somewhat different, views regarding seismicity changes

before large earthquakes have also been proposed, ranging from variations in  $b$ -values (Main 1996) to changes in intermediate size seismicity (Knopoff *et al.* 1996).

We have checked this issue on our prototype models by analysing the foreshock behaviour when approaching the mainshock. We first of all normalized each foreshock series to the ‘precursor’ time in each cluster, which for us is the number of cycles before the mainshock. We analysed the general foreshock behaviour by dividing the normalized precursor time into three time-series of the same

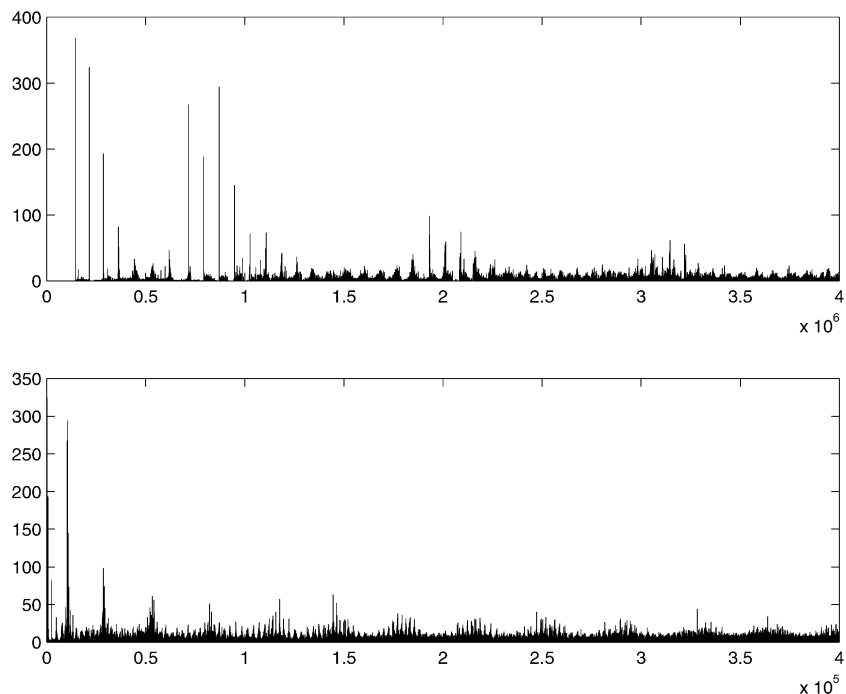


**Figure 5.** Time-series of all the events (top) and of the mainshocks only (bottom) in  $4 \times 10^6$  iterations of LDLN model. The emergence of periodic clusters of decreasing amplitude typical of highly dissipative systems is apparent.

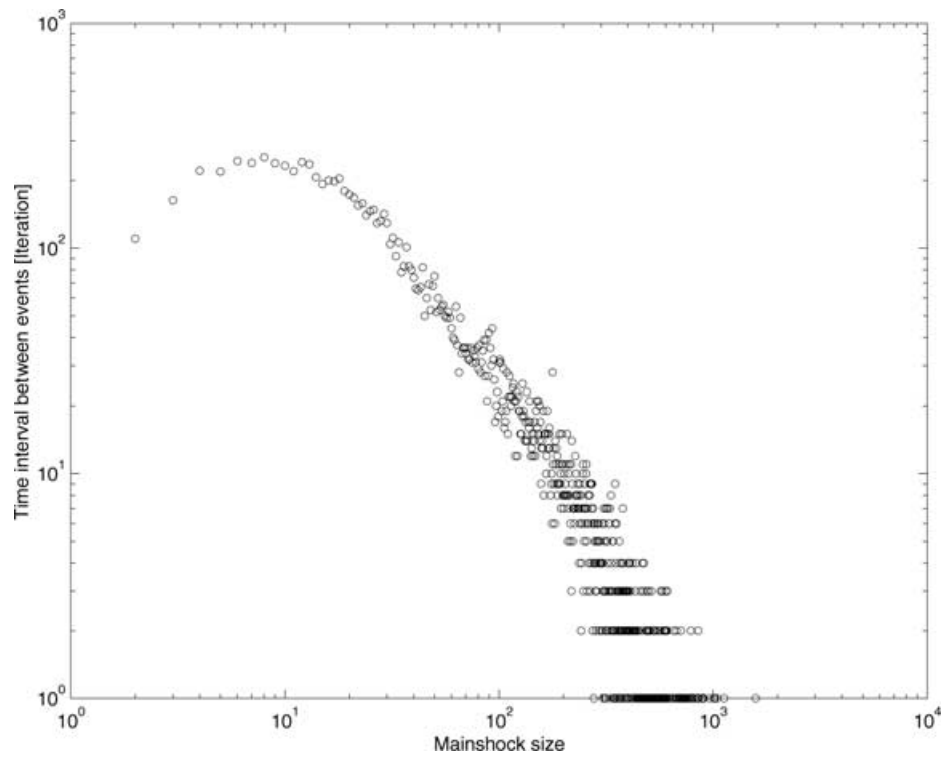


Figure 6. Distribution of the time intervals between mainshocks of comparable sizes for the LN model.

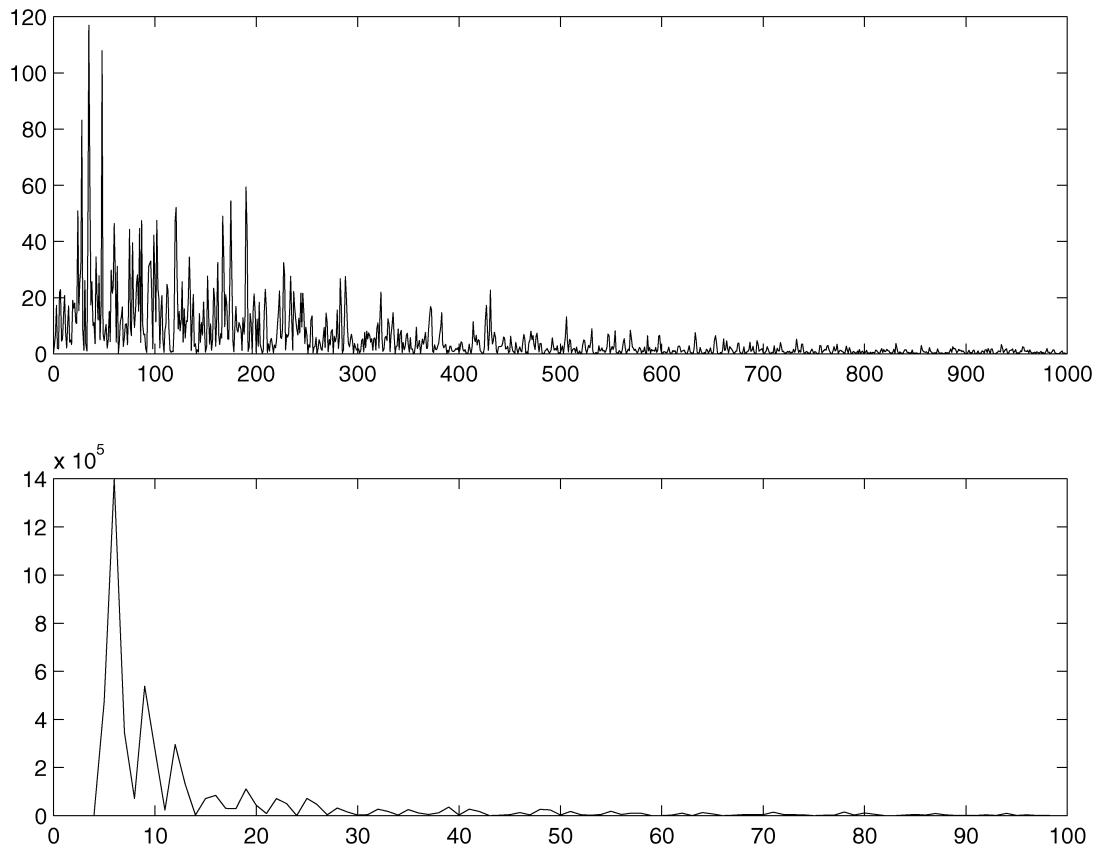
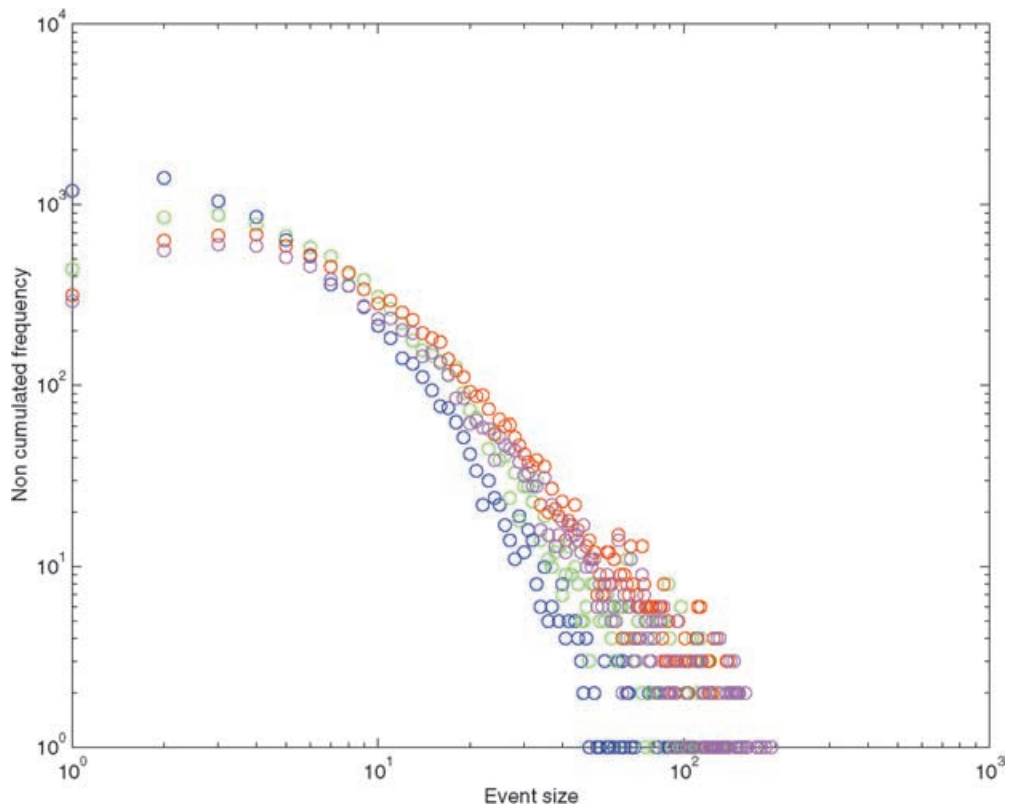
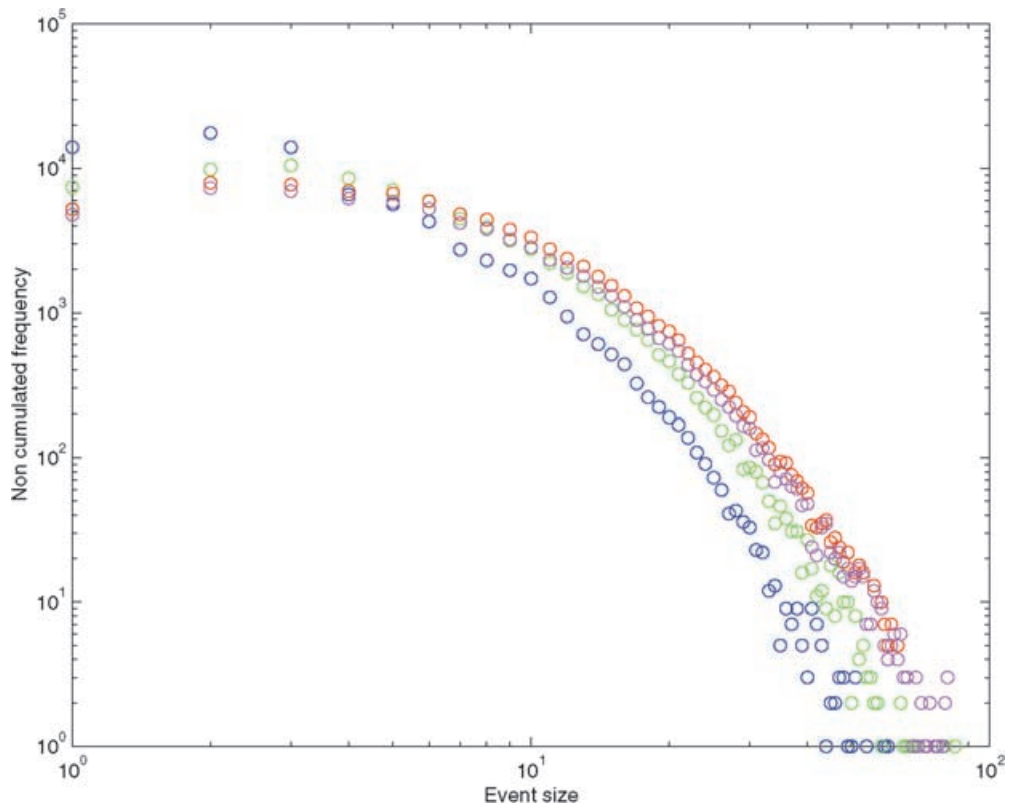


Figure 7. Power spectra of the time-series of the 20 per cent largest mainshocks. Since no significant peak arises in all the cases except the LDLNet model (bottom), the LN spectra (top) is shown for sake of comparison. Frequencies ( $x$ -axis) are expressed in  $\text{iteration}^{-1}$  units, while peak amplitude ( $y$ -axis) is in arbitrary units.



**Figure 8.** Non-cumulated distributions of the foreshocks in model SDLN, divided into classes according to their occurrence time before the mainshock. Note how this implies they coincide with the related Gutenberg–Richter distribution at the largest event size. The blue curve refers to the first 33 per cent (in time) of foreshocks, the green curve to the second 33 per cent, the red one to the third 33 per cent and the magenta one to the last 10 per cent. The cumulated distributions for all the other models show the same pattern and are therefore not reported here.



**Figure 9.** The same as Fig. 8 but for a  $600 \times 600$  grid size.



duration, starting from the events further from the mainshock and then proceeding to those closer to it. Namely, we analysed the distribution of the first (in time) 33 per cent foreshocks, of the second 33 per cent and of the last 33 per cent.

This analysis produced consistent results for all of our prototype models, and the results remained stable irrespective of the grid size and the magnitude threshold of the mainshocks. The general behaviour we found is a progressive increase in foreshock size and ‘rate of occurrence’ when approaching the mainshock. This is well apparent in the non-cumulated frequencies of occurrence of all the mainshocks (Fig. 8), and repeats itself similarly by using any lower threshold for the magnitude of the mainshocks.

Many artefacts of grid size are known (*cf.* Castellaro & Mulargia 2001) and are unavoidable owing to the limitations in computing power, so that appropriate countermeasures have been adopted for all the known effects (see above). In order to see the effect of grid size on this particular result, we have checked it on grids up to  $600^2$  cells, again finding no variation (Fig. 9).

Note how the behaviour apparent in Figs 8 and 9, with distributions at different times before the mainshocks dropping down almost parallel and progressively displaced to the right when approaching the mainshock suggests an increase in the number of events at medium to large size. Since this behaviour has been found to be stable irrespective of the magnitude of the mainshock, it implies that prior to a large event there is a decrease in the  $b$ -value

of the Gutenberg–Richter-like distribution relative to all the events. Note how only this behaviour is in agreement with what is predicted theoretically by Rundle *et al.* (1999) and apparently observed for real earthquakes by Knopoff *et al.* (1996) and Jaumé (2000).

In a broad sense, this finding supports the idea that the Earth’s crust approaches and retreats from an apparently critical state. This would also suggest that the changes in foreshock distribution, if identified correctly, could potentially signal an impending earthquake.

In conclusion, we find that, not only does the total number of foreshocks increase linearly with mainshock size (as already pointed out by Castellaro & Mulargia 2001), but also that this gain affects differently foreshocks at different times before the mainshock. Summarizing the above conclusions and also considering what emerged from our previous work (Castellaro & Mulargia 2001), we can conclude for the foreshock sequences that:

- (1) the number of foreshocks increases linearly with the mainshock dimension;
- (2) an acceleration in the rate of energy release is apparent approaching the mainshock;
- (3) the number of large events increases approaching the main event while that of small events decreases;
- (4) the large foreshocks tend to cluster near the main event.

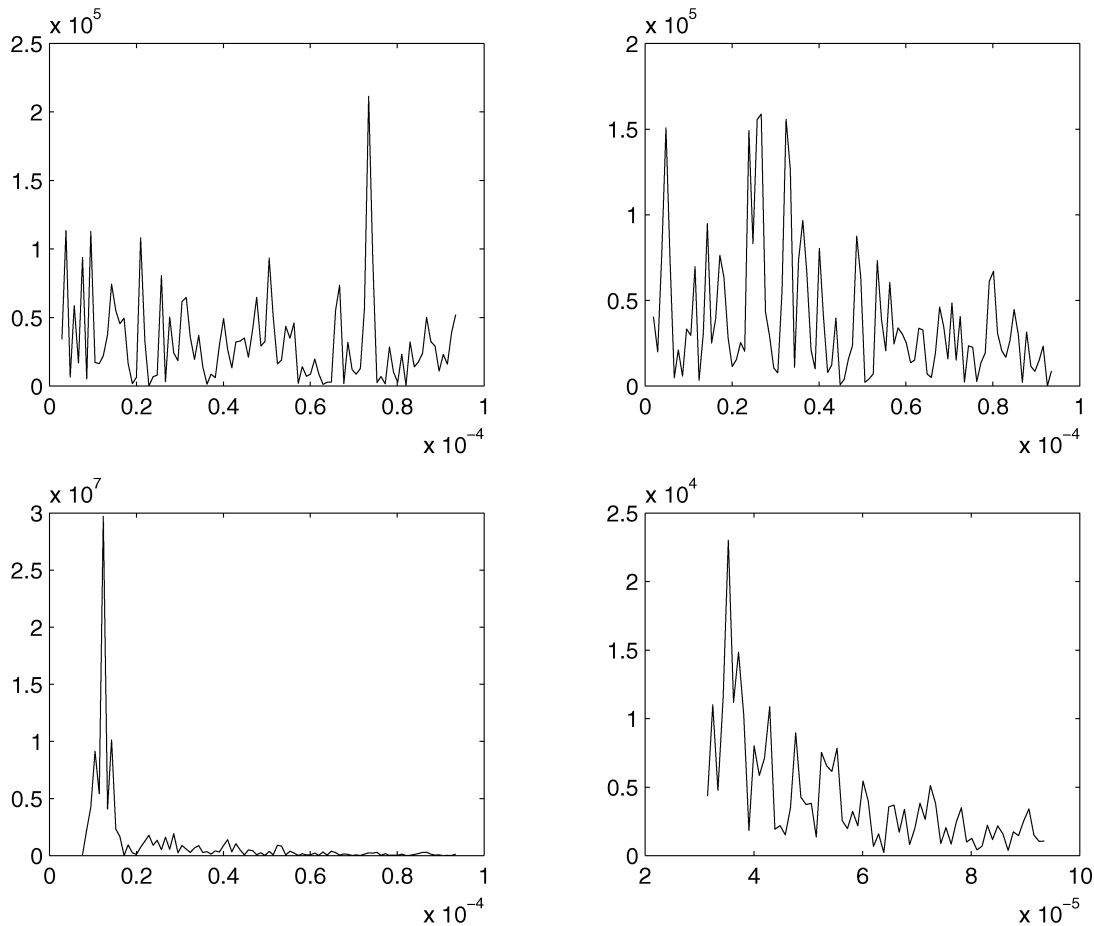


**Figure 10.** Power spectra of the time intervals between earthquakes with sizes within 20 per cent of the maximum values found for each prototype. Frequency ( $x$ -axis) is expressed in  $\text{iteration}^{-1}$  units, while peak amplitude ( $y$ -axis) is in arbitrary units. From the top left to the bottom right, the spectra show, in order, the SDLN, redSDLN, LDLN and LDLNET models.

## 6 THE SERIES OF INTEREVENT TIMES

A common question for real earthquakes is whether some periodicity exists in the recurrence times of large events. To analyse the behaviour of our prototype models with respect to this feature, we performed a spectral analysis on the time-series of event occurrences of the mainshocks divided into classes of approximately equal size. Significant peaks were found, as shown in Fig. 10, although all relative to the highly dissipative automata LDLN and LDLNET. This behaviour is similar to that of the mean energy (Fig. 1) and it could be somehow anticipated from the apparent regularity in the clustering patterns in the event series (Fig. 5).

## 7 DISCUSSION

The practical relevance and the ubiquitous presence of the Gutenberg–Richter power law has made it a candidate as the primary target for all of the cellular automata models. Most of the latter were successful in reproducing this law. This has been interpreted, in turn, as a suggestion that the Earth's is in a state of criticality or self-organized criticality. Establishing whether the Earth lithosphere is in a critical, intermittently critical or self-organized critical state would be of paramount importance for understanding the physics of earthquakes.

In this work we analysed systematically the differences in behaviour of six prototype models that we identified as the principal variants of the Bak–Tang paradigms. The first issue we investigated is the emergence of ‘criticality’ in relation to the existence of a ‘maximum correlation length’. A stable energy value was achieved by all the prototype models under stationary conditions, together with a stable maximum event size. The ‘maximum length’ was observed to be mostly affected by the cellular automaton dynamics since, under non-stationary conditions, both the average energy content and the maximum-event size were found to be systematically much larger. One could consider only the maximum values that occur under the stationary state that follows the initial transient, in which case a condition of ‘apparent criticality’, verified in a restricted range, is satisfied.

Similar interesting features emerge from our prototype models also relative to the foreshock time sequence and its distribution. The variations in the  $b$ -value of the cumulated distribution of the events preceding mainshocks of large size, shown by all the automata, seem to mirror a mechanism of preparation preceding large events. This involves an increase in foreshock size and rate of occurrence approaching each main event. If this were to occur for real earthquakes, it would indicate for a possible predictability of earthquakes. However, foreshocks are identified in retrospect for less than 20 per cent of the events and practically never in forward time (Raesenberg 1999). This demonstrates the still limited applicability of the slider-block and sand-pile cellular automata models to the real world and restrains enthusiastic attitudes towards earthquake predictability.

No periodicity in the time intervals between shocks of the same size emerged from the conservative models with long-range redistributions. This suggests that as soon as the redistribution rules become more complex, the evolution of the system becomes less regular. It may be that, although energy dissipation is a strong controlling variable, the reason it has this effect is because it tends to suppress long-range interactions.

Another interesting finding is that the realistic inclusion of local dissipation induces a periodic behaviour of the system, although one which is non-stationary and dispersive both in frequency and

amplitude. The existence of such periodicities in the real world has sometimes been suggested although never firmly established, probably because the lithosphere and the forces acting there are more complex than the slider-block-type cellular automata models.

## 8 CONCLUSIONS

Earthquake physics has recently seen a blossoming of models based on cellular automata. However, few attempts have been made to analyse them under a unified picture. In this work we studied the fundamental properties emerging from the basic variants of massless cellular automata models for earthquakes. We analysed the main different options for the geometry, the loading process and the local dissipation rules to investigate the system evolution in terms of energy, frequency-size distributions of events and periodicities.

A first problem encountered has been whether earthquake occurrence should be studied under stationary dynamics or not. The answer is not obvious for a non-conservative system such as the Earth.

As a general result, one can speak of criticality or self-organized criticality for the cellular automata models investigated only by accepting the definition of maximum-correlation length as the maximum value that appears, for the different properties investigated, under the stationary conditions following the initial transient, although the scale-invariant properties are apparent over a very limited range of scales.

A feature that emerged, common to all the models investigated, is that the foreshock number and size increase systematically before mainshocks. This is suggestive of the possibility to detect an impending mainshock. However, the fact that in the real world foreshocks can be identified in less than 20 per cent of the cases, and only in retrospect, suggests a limited applicability of the present cellular automata models.

## ACKNOWLEDGMENTS

We are grateful to Professor Ian Main and Dr Susanna Gross for their constructive suggestions. This work has been performed with the contribution of the Ministero dell'Università e della Ricerca Scientifica e Tecnologica (MURST) 40 and 60 per cent.

## REFERENCES

- Bak, P. & Tang, C., 1989. Earthquakes as a self-organized critical phenomenon, *J. geophys. Res.*, **94**, 635–637.
- Bufe, C.G. & Varnes, D.J., 1993. Predictive modeling of the seismic cycle of the Greater San Francisco Bay region, *J. geophys. Res.*, **98**, 9871–9883.
- Castellaro, S. & Mulargia, F., 2001. A simple but effective cellular automaton for earthquakes, *Geophys. J. Int.*, **144**, 609–624.
- Gutenberg, B. & Richter, C.F., 1954. *Seismicity in the Earth and Related Phenomena*, 2nd ed., Princeton University Press, Princeton.
- Jaumé, S.C., 2000. Changes in earthquake size-frequency distributions underlying accelerating seismic moment/energy release, *Geocomplexity and the Physics of Earthquakes*, pp. 199–210, eds Rundle, J.B., Turcotte, D.L. & Klein, W., AGU, Washington.
- Jaumé, S.C. & Sykes, L.R., 1999. Evolving towards a critical point: a review of accelerating seismic moment/energy release prior to large and great earthquakes, *Pure appl. Geophys.*, **155**, 279–306.
- Kinouchi, O. & Prado, C.P.C., 1999. Robustness of scale invariance in models with self-organized criticality, *Phys. Rev. E.*, **59**, 4964.
- Knopoff, L., Levishina, T., Keilis-Borok, V.I. & Mattoni, C., 1996. Increased long-range intermediate-magnitude earthquake activity prior to strong earthquakes in California, *J. geophys. Res.*, **101**, 5779–5796.

- Lomnitz-Adler, J., 1993. Automaton models of seismic fracture: constraints imposed by the magnitude–frequency relation, *J. geophys. Res.*, **98**, 17 745–17 756.
- Main, I., 1996. Statistical physics, seismogenesis and seismic hazard, *Rev. Geophys.*, **34**, 433–462.
- Main, I., O’Brien, G. & Henderson, J.R., 2000. Statistical physics of earthquakes distribution exponents for source area and potential energy and the dynamic emergence of a log-periodic energy quanta, *J. geophys. Res.*, **105**, 6105–6126.
- Raesenberg, P.A., 1999. Foreshock occurrence rates before large earthquakes worldwide, *Pure appl. Geophys.*, **155**, 355–379.
- Rundle, J.B., Klein, W. & Gross, S., 1999. Physical basis for statistical patterns in complex earthquake populations: models, predictions and tests, *Pure appl. Geophys.*, **155**, 575–607.
- Sammis, C.G. & Smith, S.W., 1999. Seismic cycles and the evolution of stress correlation in cellular automaton models of finite fault networks, *Pure appl. Geophys.*, **155**, 307–334.
- Steacy, S.J. & McCloskey, J., 1998. What controls an earthquake’s size? Results from a heterogeneous cellular automaton, *Geophys. J. Int.*, **133**, F11–F14.